Oilseed rape NAC56 transcription factor modulates reactive oxygen species accumulation and hypersensitive response-like cell death

Qinqin Chen, Fangfang Niu, Jingli Yan, Bisi Chen, Feifei Wu, Xiaohua Guo, Bo Yang* and Yuan-Qing Jiang*

State Key Laboratory of Crop Stress Biology for Arid Areas, College of Life Sciences, Northwest A & F University, Yangling, Shaanxi 712100, China

Corresponding authors, e-mail: yangwl@nwafu.edu.cn; jiangyq@nwafu.edu.cn

The NAC (NAM, ATAF1/2, CUC2) transcription factor gene family is plant-specific and plays diverse roles in development and responses to abiotic stresses and pathogen challenge. Oilseed rape (*Brassica napus*) or canola is an important oil crop worldwide, however, the function of NAC genes in it remains largely elusive. Here, we identified and characterized the NAC56 gene isolated from oilseed rape. Expression of BnaNAC56 was induced by abscisic acid (ABA), jasmonic acid (JA), methyl viologen (MV) and a necrotrophic fungal pathogen *Sclerotinia sclerotiorum*, but repressed by cold. BnaNAC56 is a transcription activator and localized to nuclei. Overexpression of BnaNAC56 induced reactive oxygen species (ROS) accumulation and hypersensitive response (HR)-like cell death, with various physiological measurements supporting these. Furthermore, BnaNAC56 expression caused evident nuclear DNA fragmentation. Moreover, quantitative reverse transcription PCR (qRT-PCR) analysis identified that the expression levels of multiple genes regulating ROS homeostasis, cell death and defense response were significantly induced. Using a dual luciferase reporter assay, we further confirmed that BnaNAC56 could activate the expression of a few ROS- and cell death-related genes. In summary, our data demonstrate that BnaNAC56 functions as a stress-responsive transcriptional activator and plays a role in modulating ROS accumulation and cell death.

This article has been accepted for publication and undergone full peer review but has not been through the copyediting, typesetting, pagination and proofreading process, which may lead to differences between this version and the Version of Record. Please cite this article as doi: 10.1111/ppl.12545

Introduction

The NAC [no apical meristem (NAM), *Arabidopsis thaliana* transcription activation factor (ATAF1/2) and cup-shaped cotyledon (CUC2)] proteins comprise one of the largest transcription factor (TF) families and are plant-specific (Olsen et al. 2005). There are 117 putative *NAC* genes in Arabidopsis and 151 in rice (Nuruzzaman et al. 2010). NAC TFs usually contain a conserved N-terminal NAC domain and highly divergent C-termini (Puranik et al. 2012). Reports have demonstrated that NAC TFs function in multiple developmental processes, including shoot apical meristem development, lateral root formation, secondary cell wall formation, hormone signal pathways and leaf senescence (Olsen et al. 2005, Puranik et al. 2012). Moreover, quite a few members of the NAC TF family also function in abiotic and biotic stress signaling and tolerance (Nakashima et al. 2012, Nuruzzaman et al. 2013). Recent evidences also reveal that some NAC TFs play a role in endoplasmic reticulum (ER) or osmotic stress-induced cell death in Arabidopsis, rice and soybean, possibly through regulating vacuolar processing enzyme (VPE) or caspase-like protein activities (Kaneda et al. 2009, Faria et al. 2011, Mendes et al. 2013, Yang et al. 2014). However, whether there are other NAC TFs regulating ROS accumulation and cell death remains unknown.

ROS are a group of free radicals derived from oxygen. The most common ROS include hydrogen peroxide (H_2O_2), singlet oxygen ($^1O_2$), superoxide radical ($O_2^{\cdot-}$) and hydroxyl radical ($OH\cdot$). ROS are produced in various subcellular compartments such as chloroplasts and mitochondria during electron transport, as well as peroxisomes via photorespiration (Apel and Hirt 2004). H_2O_2, a more stable form of ROS, can also be generated via enzymatic sources such as plasma membrane-localized NADPH oxidases (NOXs), amine oxidases, and cell wall peroxidases (Torres and Dangl 2005). Plant NOXs are also termed respiratory burst oxidase homologues (Rbohs), which constitute a small gene family and exhibit different patterns of expression and variable sensitivity to environmental factors (Sagi and Fluhr 2006). ROS are highly reactive, toxic and can lead to oxidative destruction of the cell, leaf senescence and eventual cell death. Many different kinds of environmental stresses can increase accumulation of ROS. Besides, the balance between production and elimination of ROS are disturbed by a number of abiotic factors, which may increase the intracellular levels of ROS (Suzuki et al. 2012). The redox homeostasis is the equilibrium between the production and scavenging of ROS; however, excess ROS production leads to oxidative stress (Mullineaux and Baker 2010). It is shown that oxidative stress plays an important role in

plant defense against pathogens (Yoshioka et al. 2003). Therefore, the balance between production and scavenging of ROS at the intracellular level must be tightly regulated and/or efficiently metabolized. This is very necessary to avoid potential damage caused by ROS to cellular components as well as to maintain growth, development, metabolism, and overall productivity of plants. This equilibrium between the production and detoxification of ROS is sustained by enzymatic and nonenzymatic antioxidants (Mittler et al. 2004). In plants, the major ROS-scavenging pathway is the ascorbate–glutathione cycle (AsA-GSH) in chloroplasts, cytosol, mitochondria, apoplast, and peroxisomes. This cycle, involving antioxidant enzymes such as ascorbate peroxidase (APX), monodehydroascorbate reductase (MDAR), dehydroascorbate reductase (DHAR), and glutathione reductase (GR), plays a crucial role in controlling the level of ROS in these organelles (Foyer and Noctor 2011).

During the defense response, a very efficient and immediate immune response is hypersensitive response (HR) cell death characterized by rapid, localized death of plant cells at the site of pathogen infection (Van Breusegem and Dat 2006). HR cell death is a form of programmed cell death (PCD). Abiotic stresses such as salinity, drought and heat, as well as biotic stresses like pathogen attack also induce cell death in plants, partially through affecting ROS homeostasis (Baxter et al. 2014). In addition, plant vacuoles have an important function in initiating PCD, with a key role for VPEs (Hara-Nishimura et al. 2005). Although the existence of HR cell death in plants has been known for many years (Van Hautegem et al. 2015), our knowledge of the genetic mechanisms that regulate and execute cell death is still very limited.

Oilseed rape (*Brassica napus*) is the third largest oilseed crop in the world, providing a large supply of vegetable oil. Like other crops, yield of *B. napus* seeds is greatly influenced by both abiotic and biotic stresses. In an effort to studying the roles of NAC transcription factors in stress tolerance, defense against pathogens and leaf senescence, we previously identified and cloned over 60 *NAC* genes from oilseed rape (Wang et al. 2015). In this study, we describe the characterization of one *NAC* gene, *BnaNAC56*, which could induce ROS overaccumulation and elicit cell death.

Materials and methods

Plant materials, growth condition and treatments

Oilseed rape (*Brassica napus*) seeds were surface-sterilized and sown on half-strength Murashige and Skoog (MS) medium, kept at 4°C for 2 days and then moved to a growth chamber under a daily cycle of 14 h light (150 μmol m^{-2} s^{-1})/10 h dark at 22°C. The relative humidity was 60–70%. Seven-day-old seedlings were planted in soil mix.

Sequence analysis and phylogenetic tree inference

Sequences of NAC genes were retrieved from NCBI and TAIR databases. Multiple sequence alignment was performed using ClustalX1.83 program using translated amino acid sequences. A phylogenetic tree was generated by MEGA6 software using the maximum parsimony (MP) algorithm with 1000 replications.

Transcriptional activity assay

The coding region of *BnaNAC56* gene was cloned into the pYJHA vector using the primers listed in Table S1. The assay was performed as described previously (Niu et al. 2016).

Quantitative RT-PCR (qRT-PCR) assay

Stress and hormone-treated oilseed rape tissues of three independent biological replicates were prepared as described previously (Niu et al. 2014). Total RNA was extracted from frozen samples using Plant RNA kit (Omega Bio-tek, Norcross, GA). First-strand cDNAs were synthesized from 2.5 μg of total RNA as described previously (Liang et al. 2013). qRT-PCR was performed using diluted cDNAs and SYBR Green I premix (CWBio, Beijing, China) on a CFX96 real-time PCR system (Bio-Rad, Hercules, CA). The specificity and amplification efficiency of each pair of primers (Table S1) were assayed before use. Extraction of RNA from *N. benthamiana* leaf discs was performed as described above, again from three biological replicates. *BnaUP1* and *BnaUBC9* (oilseed rape) and *NbPP2A*, *NbL23* and *NbF-box* (*N. benthamiana)* were used as internal control to normalize the data. Two technical replicates for each of the three biological replicates were run and the significance was determined using a *t*-test in SPSS statistical

software ($P \leq 0.05$).

Subcellular localization determination

The coding region of *BnaNAC56* was amplified using a pair of gene-specific primers (Table S1) and *Pfu* polymerase (Bioer, Hangzhou, China) before inserted into the vector pYJGFP, yielding plasmid pYJGFP-BnaNAC56. This plasmid and the pYJGFP vector were transformed into *Agrobacterium tumefaciens* GV3101 before infiltrated separately into leaves of 28-d-old *N. benthamiana* using 1 ml needleless syringes (Liang et al. 2013). 48 h later, GFP signals were excited at 488 nm and detected on a LSM510 Meta laser scanning confocal microscope (Zeiss, Oberkochen, Germany).

Overexpression and physiological measurements

The coding region of *BnaNAC56* or *GFP* was subcloned into the binary vector pYJHA using primers listed in Table S1. Agroinfiltration into the lower epidermal side of 30 day old leaves of *N. benthamiana* plants were performed as described previously (Sun et al. 2014). Electrolyte leakage was measured according to (Sun et al. 2014). Qualitative and quantitative assays of hydrogen peroxide (H_2O_2) were performed as previously described (Sun et al. 2014, Chen et al. 2016). Quantitative assays of chlorophyll, anthocyanin and malondialdehyde (MDA) were performed as previously described (Niu et al. 2014, Niu et al. 2016).

TUNEL assay

In situ nick-end labeling of nuclear DNA fragmentation was performed using the Dead End Fluorometric TUNEL system according to the manufacturer's instructions (Promega, Madison, WI). Samples were observed on a confocal laser scanning microscope (A1R, Nikon, Tokyo, Japan) using a 488 nm excitation wavelength for fluorescein and a 460 nm excitation wavelength for DAPI as described previously (Niu et al. 2016).

Transient expression in protoplasts and expression analysis during leaf senescence in oilseed rape

The coding regions of *BnaNAC56*, *GFP* and *GUS* control were subcloned individually into pUC19 as described previously (Wang et al. 2015). Protoplast isolation and transfection were performed as described

previously (Wang et al. 2015). The Evans blue and fluorescein diacetate (FDA) stainings were performed as described previously (Niu et al. 2016). Scoring of protoplasts was performed with a fluorescence microscope (BX53, Olympus, Tokyo, Japan). The dead rates of protoplasts were determined by assaying 20 independent samples. Detection of ROS level in protoplasts was carried out using fluorescent dye 2',7'-dichlorodihydrofluorescein diacetate (H_2DCFDA, Sigma-Aldrich, Saint Louis, MO). Briefly, the freshly protoplasts were incubated in a staining buffer (10 m*M* Tris, 50 m*M* KCl, pH 7.2, 25 μ*M* H_2DCFDA) for 10 min at 25°C in the dark. After washing, fluorescence was examined using a fluorescence microscope (BX53, Olympus, Tokyo, Japan) with excitation at 488 nm and emission at 525 nm. All images were taken under identical conditions. Leaves of soil-grown oilseed rape plants at different stages were harvested and RNA was extracted using Trizol (Sangon, Shanghai, China) for qRT-PCR assay. Three biological replications were performed.

Dual luciferase reporter assay

To generate reporter constructs, the promoters were amplified from genomic DNA and cloned into the pGreen II 0800-LUC vector, using the primers listed in Table S1. To generate effector constructs, *BnaNAC56* or *GFP* was subcloned into the pYJHA vector. The *Renilla* luciferase (REN) under the control of the 35S promoter contained in the reporter construct was used as the endogenous control. Dual LUC assay was performed as described previously (Hellens et al. 2005). Firefly and *Renilla* luciferase activities were quantified using Dual-Luciferase Reporter Assay System (Promega, Madison, WI) and detected with GloMax 20/20 Luminometer (Promega, Madison, WI) according to the manufacturer's instructions. Three independent measurements were made for each construct combination.

Statistical analysis

Each experiment was repeated three times independently. Data were statistically analyzed by using SPSS 16.0 software.

Results

Identification, cloning and analysis of *BnaNAC56* gene

Previously, a NAC gene showing high identity to *ANAC056* in Arabidopsis was cloned from oilseed rape (*B. napus*) and designated as *BnaNAC56*. The *BnaNAC56* encodes a protein with 351 amino acid residues, which contains a typical NAC domain divided into five highly conserved subdomains, namely A, B, C, D and E (Fig. 1A). In addition, a short motif rich in basic amino acids was present in the subdomain D, and this motif is the putative nuclear localization signal (NLS) (Fig. S1).

Phylogenetic analysis showed that BnaNAC56 is closely related to ANAC056 (AtNAC2/NARS1, At3g15510) and ONAC010 (Os07g37920), showing an identity of 92.6 and 50.9% at amino acid level, respectively. As NAC TFs are specific to plants, we traced the origin of *BnaNAC56* in land plants. To this end, a total of 32 *NAC* genes were identified from the non-vascular plant, *Physcomitrella patens* and, 20 *NAC* genes from the first vascular plant, *Selaginella moellendorffii* (Table S2). As shown in Fig. 1B, BnaNAC56 and a few NAC from Arabidopsis and rice formed an independent clade in the tree in which no NAC from *P. patens* or *S. moellendorffii* is present, suggesting that BnaNAC56 may have emerged rather later in the evolutionary history.

Expression of *BnaNAC56* responds to multiple stress treatments

To explore the possible involvement of *BnaNAC56* in abiotic stress and hormone responses as well as a devastating fungal pathogen *S. sclerotiorum* challenge, we analyzed the expression pattern of it using qRT-PCR. The results revealed that the expression of *BnNAC56* was rapidly and significantly induced by ABA, JA, SA, MV and *S. sclerotiorum* within 1 h (Fig. 1C). However, cold treatment down-regulated the expression of *BnaNAC56* at the 1 h time-point. These data suggest that *BnaNAC56* may play a role in plant response to these phytohormones and infection of the necrotrophic fungal pathogen.

BnaNAC56 is nucleus-localized transcriptional activator

To investigate the subcellular localization of BnaNAC56, expression plasmids carrying *GFP* and *BnaNAC56-GFP* under the control of CaMV35S promoter were introduced to leaf cells of *N. benthamiana*. The results showed that GFP was detected in the nucleus and cytosol, whereas BnaNAC56-GFP was

detected only in the nucleus (Fig. 2A). Thus, we concluded that the BnaNAC56 protein is targeted to the nucleus.

The activity of BnaNAC56 as a transcriptional regulator was assayed using a LUC-based chimeric effector/reporter system (Fig. 2B). The reporter plasmid 3xNACRS-LUC was co-expressed with an effector plasmid carrying either *BnaNAC56* or the *GFP* control. The relative ratio of LUC to REN was significantly increased when *BnaNAC56* was expressed compared with *GFP* (Fig. 2C), indicating the BnaNAC56 acts as a transcriptional activator through binding to the canonical NACRS element.

BnaNAC56 expression induces ROS accumulation and hypersensitive response-like cell death

In the previous subcellular localization assay, we observed significant water-soaking symptom in the infiltrated area expressing *BnaNAC56.* Therefore, we initiated further experiments to investigate whether the newly identified BnaNAC56 possessed cell death-inducing activity. In this regard, we performed overexpression of *BnaNAC56* and *GFP* control. Consistent with the previous observation, overexpression of *BnaNAC56* induced pathogen-independent cell death in the infiltrated area, whereas *GFP* did not (Fig. 3A). An immunoblot analysis indicates that both *GFP* and *BnaNAC56* were expressed in the respective leaf tissues after agroinfiltration at three time-points (Fig. S2). As oxidative burst induced by ROS plays a role in plant defense response and cell death, we explored the role of ROS in BnaNAC56-induced cell death. As a result, significant hydrogen peroxide (H_2O_2) production was detected in the infiltrated areas, indicated by a characteristic brown color through 3,3'-diaminobenzidine (DAB) staining. A quantitative assay of H_2O_2 content showed that there was more H_2O_2 in leaf tissues expressing *BnaNAC56* than that of *GFP*, beginning at 5 dpi and proceeding as expected (Fig. 3B). Furthermore, when the extent of cell death was measured via an ion leakage assay, significantly increased ion leakage was detected with the *BnaNAC56*-overexpressing tissue, compared to the *GFP* control (Fig. 3C).

As the lipid peroxidation product, malondialdehyde (MDA) is an important indicator of oxidative damage. MDA contents increased in the *BnaNAC56*-overexpressing tissues when compared with the *GFP* (Fig. 4A). A quantitative comparison of chlorophyll contents showed expression of *BnaNAC56* caused a significant decrease of chlorophyll compared to *GFP* control beginning at 3 dpi (Fig. 4B). In contrast, the anthocyanin concentration in the tissue expressing *BnaNAC56* significantly increased beginning at 5 dpi,

whereas no significant change was observed in leaf tissues expressing the *GFP* gene (Fig. 4C).

As DNA fragmentation is a PCD marker, we used the TUNEL assay to detect single- and double-strand DNA breaks of epidermal cells. Confocal microscopy showed strong fluorescent staining in the epidermal nuclei of the *BnaNAC56*-expressing tissue at 5 dpi, indicative of single- or double-stranded DNA breaks in the nuclei (Fig. 5A). In contrast, signal was not detected in the *GUS* expression tissue (Fig. 5B). A DNA laddering assay also confirmed that genomic DNA degradation was obvious in *BnaNAC56*-expressing tissues (Fig. S3).

Expression of *BnaNAC56* induced ROS accumulation and cell death of protoplasts and showed preferential expression in senescent leaves

To determine the function of BnaNAC56, we also introduced *BnaNAC56* expression plasmids into isolated protoplasts of oilseed rape, with *GFP* or *GUS* expression plasmids as the control, depending on the type of fluorescent dyes used. By using a fluorescence dye, H_2DCFDA, we found that protoplasts transfected with *BnaNAC56*-containing plasmids accumulated more ROS than those of control (Fig. 6A). An Evans blue staining showed 19.4% of protoplasts transfected with *BnaNAC56* were dead, compared to 5.8% in the control (Fig. 6B–C). A further FDA staining confirmed that a large portion (21.0%) of *BnaNAC56*-transfected protoplasts was dead, whereas only 3.1% of protoplasts expressing the *GUS* gene were dead (Fig. 6D–E). These assays demonstrated that BnaNAC56 TF indeed positively regulates ROS accumulation and cell death.

As leaf senescence is a developmentally programmed cell death process and ROS accumulation can lead to premature leaf senescence, we further examined the expression pattern of *BnaNAC56* during leaf senescence in oilseed rape. Samples of young leaves (YL), mature leaves (ML), early senescent leaves (ES) and late senescent leaves (LS) as well as different sections of early senescent leaves were harvested for qRT-PCR assay. The data revealed that, compared with YL, the expression of *BnaNAC56* was prominently higher in LS than in any other leaf tissues (Fig. 6F).

Expression profiling of ROS-, cell death- and defense-related genes

Considering the fact that *BnaNAC56* overexpression induced ROS accumulation and cell death, we next

sought to determine how BnaNAC56 exerts its role in these processes by investigating the expression profiles of an array of marker genes through qRT-PCR. Firstly, the expression levels of two genes encoding Rboh responsive for apoplastic ROS production were examined. The result showed that only *RbohA* was slightly up-regulated (1.4 fold) at 3 dpi, and *RbohB* was not significantly changed at the two time-points investigated (Fig. 7A). Next, the transcript levels of three genes encoding vacuolar processing enzymes (VPEs), which are cysteine proteinase responsible for the maturation of vacuolar proteins and have caspase-1-like activity (Hatsugai et al. 2004), were compared between *BnaNAC56*- and *GFP*-expressing tissues. Besides, two metacaspase genes, *MC4* and *MC8*, which encode cysteine proteases structurally related to caspases in animals, were also included in the analysis. Interestingly, our data revealed that expression of *VPE1a, VPE1b* and *VPE3* were all up-regulated at 2 and 3 dpi, with the induction of *VPE1a* and *VPE3* significant (Fig. 7A). Surprisingly, expression of *MC4* and *MC8* was slightly down-regulated by *BnaNAC56* expression (Fig. 7A). Thirdly, we examined the changes in transcript abundance of a few genes encoding ROS-scavenging enzymes, including ascorbate peroxidase (APX), catalase (CAT), glutathione peroxidase (GPX), glutathione S-transferase (GST) and superoxide dismutase (SOD) (Apel and Hirt 2004) as well as alternative oxidase (AOX) implicated in lowering ROS content in mitochondria (Maxwell et al. 1999). The results showed that expression of *CAT3* and *GST1* were predominantly induced by *BnaNAC56* expression, while that of the *APX1*, *APX4*, *tAPX*, *CAT1* and *SOD* were significantly down-regulated at one or two time-points. The expression of other ROS-scavenging genes and *AOX1a* did not show any significant change, which suggests that they may not act directly downstream of BnaNAC56 TF. Fourthly, the expression of two marker genes of leaf senescence was examined and they are *senescence-associated gene* (*SAG*) *12* and *SAG101*, encoding a cysteine protease and an acyl hydrolase, respectively (Balazadeh et al. 2008). Unexpectedly, expression of these two *SAG* genes did not show significant change (Fig. 7B). We further examined the expression levels of *ethylene-insensitive 2* (*EIN2*) and *ethylene response factor 102* (*ERF102*), which are marker genes of ethylene promoting leaf senescence. We found that both of them were down-regulated. Besides, a C2H2-type zinc finger transcription factor gene coding for ZAT12 was monitored. Previous studies show that ZAT12 is required for the up-regulation of ROS-related genes *APX1*, *ZAT7* and *WRKY25* (Davletova et al. 2005). However, *ZAT12* level was not significantly changed in the tissue undergoing ROS

accumulation and cell death.

Finally, as ROS play a positive role in plant defense against pathogens and HR-like cell death is commonly associated with immune responses (De Pinto et al. 2012), we further monitored the expression of representative genes involved in plant defense responses. The results showed that expression of *ACRE31*, *ACRE132*, *CP23* and *CYP71D20* were down- regulated at 2 and 3 dpi, respectively (Fig. 7B). At the same time, expression of *HIN1* (*harpin inducing 1*), *pathogenesis-related* (*PR*)*2* and *PR5* were induced in *BnaNAC56*-expressing tissues at one or two time-points investigated, although some of the changes are not very significant as a result of large error bars (Fig. 7B).

In view of the fact that BnaNAC56 is a transcriptional activator, we therefore tested the transcriptional regulation between BnaNAC56 and up-regulated marker genes using a dual LUC assay system. For this goal, we cloned the ca. 1 kb promoter fragments of two up-regulated genes and fused them upstream of *LUC* gene and CaMV35S promoter-driven *REN* was used as the internal control. The effector plasmids contain either *BnaNAC56* or *GFP* expression cassette (Fig. 8A). The reporter and effector plasmids were then introduced to express corresponding proteins via agroinfiltration. The ability of BnaNAC56 to transcriptionally activate its putative downstream genes was calculated through LUC/REN ratios. As shown in Fig. 8B, *BnaNAC56* expression activated the LUC activity under the control of *VPE1a*, *GST1* and *HIN1* promoters.

Discussion

The NAC gene family is plant-specific and functional characterization of NAC genes in model plants demonstrates that they play diverse roles, in development, secondary cell wall formation, leaf senescence and fruit ripening, as well as in tolerance of biotic and abiotic stresses (Puranik et al. 2012, Nuruzzaman et al. 2013). In general, NAC TFs could act as either activators or repressors of gene expression. We now know that HR-like cell death can be a result of overexpression of certain genes in plants, and initiation of it requires de novo protein synthesis, which suggests that HR cell death is induced by a transcriptional network involving some key transcription factors (Kaneda et al. 2009). So far, only a few NAC genes from Arabidopsis and rice have been reported to regulate cell death or leaf/fruit senescence (Kaneda et al. 2009, Faria et al. 2011, Woo et al. 2013, Yang et al. 2014). We still have very limited evidences if there is

any NAC TF(s) regulating ROS burst-dependent cell death.

Oilseed rape is a very important oil crop, however, the function of NAC genes in it remains largely elusive. In this study, we characterized *NAC56* transcription factor gene isolated from oilseed rape, as a component of ROS and cell death signaling pathway. *BnaNAC56* encodes a stress-responsive and plant-specific NAC protein acting as a transcriptional activator (Figs. 1–2). Overexpression of *BnaNAC56* leads to significant ROS accumulation, which was indicated by DAB staining and remarkable lipid peroxidation and so on (Figs 3 and 4). At the same time, HR-like cell death occurred accompanied by the loss of integrity of plasma membrane and nuclear DNA fragmentation specific to HR cell death (Fig. 5). In addition, *BnaNAC56* expression was found to induce ROS accumulation and cell death of protoplasts of oilseed rape (Fig. 6), which is similar to rice *NAC4* (Kaneda et al. 2009). Interestingly, we found that BnaNAC56 induced the expression of caspase-1-like VPEs, which have been shown to play a crucial role in cell death program (Hara-Nishimura et al. 2005). Arabidopsis VPE genes could be classified into two types: seed-type and vegetative-type. Seed-type VPEs are responsible for the conversion of proproteins of vacuole into mature forms, and the vegetative-type VPEs play a role in cell death (Lam 2005). A study proved that virus-induced gene silencing (VIGS) of *VPE1a* and *VPE1b* inhibit hypersensitive cell death in *N. benthamiana* (Hatsugai et al. 2004). Since vacuole-triggered cell death is unique to plants, it is not surprising that a plant-specific NAC56 protein serves as a regulatory circuit leading to the activation of *VPEs*. A bioinformatic analysis and literature scanning indicated that ortholog of *BnaNAC56* in the closest relative Arabidopsis has not reported to induce ROS accumulation or HR-like cell death yet. In summary, this study work showed that *BnaNAC56* is a novel member in the family of NAC TFs that induced ROS accumulation and HR-like cell death.

Author contributions

Conceived and designed the experiments: YQJ, BY. Performed the experiments: QC, FN, JY. Analyzed the data: YQJ, QC, BY. Contributed materials: BC, FW, XG. Wrote the paper: YQJ.

Acknowledgements – This study was supported by the Fundamental Research Funds for the Central Universities (2452016080 to YQJ and 2452015413 to BY), the Natural Science Foundation of Shaanxi

Province (2015JM3076 to YQJ and 2014JQ3102 to BY). We thank prof. Jian-Ye Chen (South China Agricultural University) for providing the LUC vector.

References

Apel K, Hirt H (2004) Reactive oxygen species: metabolism, oxidative stress, and signal transduction. Annu Rev Plant Biol 55: 373–399

Balazadeh S, Riano-Pachon DM, Mueller-Roeber B (2008) Transcription factors regulating leaf senescence in *Arabidopsis thaliana*. Plant Biol (Stuttg) 10 Suppl 1: 63–75

Baxter A, Mittler R, Suzuki N (2014) ROS as key players in plant stress signalling. J Exp Bot 65: 1229–1240

Chen B, Niu F, Liu WZ, Yang B, Zhang J, Ma J, Cheng H, Han F, Jiang YQ (2016) Identification, cloning and characterization of R2R3-MYB gene family in canola (*Brassica napus* L.) identify a novel member modulating ROS accumulation and hypersensitive-like cell death. DNA Res 23: 101–114

Davletova S, Schlauch K, Coutu J, Mittler R (2005) The zinc-finger protein Zat12 plays a central role in reactive oxygen and abiotic stress signaling in Arabidopsis. Plant Physiol 139: 847–856

De Pinto MC, Locato V, De Gara L (2012) Redox regulation in plant programmed cell death. Plant Cell Environ 35: 234–244

Faria JA, Reis PA, Reis MT, Rosado GL, Pinheiro GL, Mendes GC, Fontes EP (2011) The NAC domain-containing protein, GmNAC6, is a downstream component of the ER stress- and osmotic stress-induced NRP-mediated cell-death signaling pathway. BMC Plant Biol 11: 129

Foyer CH, Noctor G (2011) Ascorbate and glutathione: the heart of the redox hub. Plant Physiol 155: 2–18

Hara-Nishimura I, Hatsugai N, Nakaune S, Kuroyanagi M, Nishimura M (2005) Vacuolar processing enzyme: an executor of plant cell death. Curr Opin Plant Biol 8: 404–408

Hatsugai N, Kuroyanagi M, Yamada K, Meshi T, Tsuda S, Kondo M, Nishimura M, Hara-Nishimura I (2004) A plant vacuolar protease, VPE, mediates virus-induced hypersensitive cell death. Science 305: 855–858

Hellens RP, Allan AC, Friel EN, Bolitho K, Grafton K, Templeton MD, Karunairetnam S, Gleave AP,

Laing WA (2005) Transient expression vectors for functional genomics, quantification of promoter activity and RNA silencing in plants. Plant Methods 1: 13

Kaneda T, Taga Y, Takai R, Iwano M, Matsui H, Takayama S, Isogai A, Che FS (2009) The transcription factor OsNAC4 is a key positive regulator of plant hypersensitive cell death. EMBO J 28: 926–936

Lam E (2005) Vacuolar proteases livening up programmed cell death. Trends Cell Biol 15: 124–127

Liang W-W, Yang B, Yu B-J, Zhou Z-Z, Li C, Sun Y, Zhang Y, Jia M, Wu F-F, Zhang H-F, Wang B-Y, Deyholos M, Jiang Y-Q (2013) Identification and analysis of MKK and MPK gene families in Canola (*Brassica napus* L.). BMC Genomics 14: 392

Maxwell DP, Wang Y, McIntosh L (1999) The alternative oxidase lowers mitochondrial reactive oxygen production in plant cells. Proc Natl Acad Sci USA 96: 8271–8276

Mendes GC, Reis PA, Calil IP, Carvalho HH, Aragao FJ, Fontes EP (2013) GmNAC30 and GmNAC81 integrate the endoplasmic reticulum stress- and osmotic stress-induced cell death responses through a vacuolar processing enzyme. Proc Natl Acad Sci USA 110: 19627–19632

Mittler R, Vanderauwera S, Gollery M, Van Breusegem F (2004) Reactive oxygen gene network of plants. Trends Plant Sci 9: 490–498

Mullineaux PM, Baker NR (2010) Oxidative stress: antagonistic signaling for acclimation or cell death? Plant Physiol 154: 521–525

Nakashima K, Takasaki H, Mizoi J, Shinozaki K, Yamaguchi-Shinozaki K (2012) NAC transcription factors in plant abiotic stress responses. Biochim Biophys Acta 1819: 97–103

Niu F, Wang B, Wu F, Yan J, Li L, Wang C, Wang Y, Yang B, Jiang YQ (2014) Canola (*Brassica napus* L.) NAC103 transcription factor gene is a novel player inducing reactive oxygen species accumulation and cell death in plants. Biochem Biophys Res Commun 454: 30–35

Niu F, Wang C, Yan J, Guo X, Wu F, Yang B, Deyholos M, Jiang YQ (2016) Functional characterization of NAC55 transcription factor from oilseed rape (*Brassica napus* L.) as a novel transcriptional activator modulating reactive oxygen species accumulation and cell death. Plant Mol Biol 92: 89–104

Nuruzzaman M, Manimekalai R, Sharoni AM, Satoh K, Kondoh H, Ooka H, Kikuchi S (2010) Genome-wide analysis of NAC transcription factor family in rice. Gene 465: 30–44

Nuruzzaman M, Sharoni AM, Kikuchi S (2013) Roles of NAC transcription factors in the regulation of

biotic and abiotic stress responses in plants. Front Microbiol 4: 248

Olsen AN, Ernst HA, Leggio LL, Skriver K (2005) NAC transcription factors: structurally distinct, functionally diverse. Trends Plant Sci 10: 79–87

Puranik S, Sahu PP, Srivastava PS, Prasad M (2012) NAC proteins: regulation and role in stress tolerance. Trends Plant Sci 17: 369–381

Sagi M, Fluhr R (2006) Production of reactive oxygen species by plant NADPH oxidases. Plant Physiol 141: 336–340

Sun Y, Wang C, Yang B, Wu F, Hao X, Liang W, Niu F, Yan J, Zhang H, Wang B, Deyholos M, Jiang Y-Q (2014) Identification and functional analysis of mitogen-activated protein kinase kinase kinase (MAPKKK) genes in canola (*Brassica napus* L.). J Exp Bot 65: 2171–2188

Suzuki N, Koussevitzky S, Mittler R, Miller G (2012) ROS and redox signalling in the response of plants to abiotic stress. Plant Cell Environ 35: 259–270

Torres MA, Dangl JL (2005) Functions of the respiratory burst oxidase in biotic interactions, abiotic stress and development. Curr Opin Plant Biol 8: 397–403

Van Breusegem F, Dat JF (2006) Reactive oxygen species in plant cell death. Plant Physiol 141: 384–390

Van Hautegem T, Waters AJ, Goodrich J, Nowack MK (2015) Only in dying, life: programmed cell death during plant development. Trends Plant Sci 20: 102–113

Wang B, Guo X, Wang C, Ma J, Niu F, Zhang H, Yang B, Liang W, Han F, Jiang YQ (2015) Identification and characterization of plant-specific NAC gene family in canola (*Brassica napus* L.) reveal novel members involved in cell death. Plant Mol Biol 87: 395–411

Woo HR, Kim HJ, Nam HG, Lim PO (2013) Plant leaf senescence and death – regulation by multiple layers of control and implications for aging in general. J Cell Sci 126: 4823–4833

Yang ZT, Wang MJ, Sun L, Lu SJ, Bi DL, Sun L, Song ZT, Zhang SS, Zhou SF, Liu JX (2014) The membrane-associated transcription factor NAC089 controls ER-stress-induced programmed cell death in plants. PLoS Genet 10: e1004243

Yoshioka H, Numata N, Nakajima K, Katou S, Kawakita K, Rowland O, Jones JD, Doke N (2003) *Nicotiana benthamiana* gp91phox homologs NbrbohA and NbrbohB participate in H_2O_2 accumulation and resistance to *Phytophthora infestans*. Plant Cell 15: 706–718

Supporting information

Additional Supporting Information may be found in the online version of this article:

Table S1. Primers used in this study.

Table S2. List of NAC genes for the phylogenetic analysis.

Fig. S1. Multiple sequence alignment BnaNAC56 with typical NAC proteins.

Fig. S2. Immunoblot assay of protein expression.

Fig. S3. DNA laddering assay.

Edited by E. Pesquet

Figure legends

Fig. 1. Sequence and expression analysis of oilseed rape *NAC56*. (A) Domain analysis of BnaNAC56. The N-terminal NAC domain and C-terminal transcriptional regulatory (TR) domain are shown, with the former divided into five conserved subdomains (A–E; shown in gray boxes). (B) Phylogenetic analysis of BnaNAC56. The tree was constructed using the maximum parsimony method implemented in MEGA6 based on amino acid sequences with BnaNAC56 indicated by a diamond. The numbers on the nodes are percentages from a bootstrap analysis of 1000 replicates. Os, *Oryza sativa*; Pp, *Physcomitrella patents*; Sm, *Selaginella moellendorffi*. (C) qRT-PCR analysis of *BnaNAC56* in response to various treatments. Data is the mean of three biological replicates ± S.E. Asterisks denote significant differences (compared to 1) by Student *t*-test analysis (* $P \leq 0.05$; ** $P \leq 0.01$).

Fig. 2. Subcellular localization and transactivational activity and of BnaNAC56. (A) Subcellular localization of BnaNAC56-GFP and GFP proteins in *N. benthamiana* cells. The left is GFP fluorescence, the middle bright field and the right an overlay of the two images. Bar = 50 μm. (B) Effect of BnaNAC56 on firefly luciferase (LUC) gene expression controlled by triple tandem repeats of NACRS element as revealed by dual LUC assay. GFP is the control. Asterisks denote significant differences by Student *t*-test analysis (** $P \leq 0.01$).

Fig. 3. Overexpression of *BnaNAC56* induced ROS accumulation and HR-like cell death. (A) Cell death phenotype of *N. benthamiana* leaves. The diagram on the top represents the positions of infiltrated samples. The phenotype was monitored for several days post-infiltration (dpi). The left, middle and right columns represent the front, back sides and DAB staining, respectively. (B–C) Quantitative comparison of electrolyte leakages and hydrogen peroxide contents at various time-points, respectively. Values represent the means of three independent assays for each time-point ± S.E. Identical and different letters represent non- and significant differences ($P \leq 0.05$).

Fig. 4. Quantitative comparison of physiological indexes between *BnaNAC56*- and GFP-expressing

tissues. (A–C) Quantification of MDA, chlorophyll and anthocyanin contents in leaf tissues expressing *BnaNAC56* or *GUS* at various time-points. Each value is means of three independent assays ± S.E. Identical and different letters represent non- and significant differences ($P \leq 0.05$).

Fig. 5. Confocal images of the TUNEL assay of nuclear DNA fragmentation induced by *BnaNAC56* expression. (A) and (B), Images of leaves expressing *BnaNAC56* and *GUS* at 5 dpi, respectively. Leaves were counterstained with DAPI. Scale bar = 20 μm.

Fig. 6. Expression of *BnaNAC56* in protoplasts of oilseed rape induced ROS accumulation and cell death. (A) Detection of ROS through the fluorescent H_2DCFDA dye. Protoplasts were transfected with the pUC19-BnaNAC56 and pUC19-GUS (control) plasmids, respectively. After 18 h, ROS of protoplasts was detected with H_2DCFDA. Red circles indicate protoplasts without detectable fluorescence. Bar = 50 μm. (B) Examination of cell death through Evans blue staining. The red arrow and circle indicate a dead protoplast. Bar = 100 μm. (C) Percentages of dead protoplasts. Data are presented as mean ± S.E (n = 20). ** $P \leq 0.01$ (student's *t*-test). (D) Investigation of cell viability through FDA staining. The red arrow and circle indicate a dead protoplast. Bar = 100 μm. (E) Percentages of dead protoplasts as detected by FDA staining. Data are presented as mean ± S.E (n = 22). ** $P \leq 0.01$ (student's *t*-test). (F) qRT-PCR analysis of *BnaNAC56* expression during leaf senescence. YL, young leaves; ML, mature leaves; ES, early senescent leaves; LS, late senescent leaves; T, M and B indicate tip, middle and base of ES senescent leaves. Data is the mean of three biological replicates ± S.E.

Fig. 7. qRT-PCR analysis of transcript abundance of ROS-, cell death- and defense-related marker genes. (A) and (B) qRT-PCR was performed to determine transcript levels of marker genes in control and *BnaNAC56*-expressing leaves at 2 and 3 dpi. Each value represents the mean ± S.E. of three biological replicates. Asterisks denote significant differences (compared to 1) by Student *t*-test analysis (* $P \leq 0.05$; ** $P \leq 0.01$).

Fig. 8. The dual luciferase reporter assay of transcription activation of BnaNAC56. (A) Schematic

representation of the double-reporter and effector plasmids used in the dual LUC assay. The double-reporter plasmid contains the respective promoter regions fused to LUC and *Renilla* (REN) luciferase driven by CaMV35S. The effector plasmid contains the *BnaNAC56* driven by the CaMV35S. TL, translational leader sequence from tobacco etch virus; Ter, NOS terminator. (B) Ability of BnaNAC56 to activate expression of LUC under the control of various promoter regions. The activities of LUC and REN were measured sequentially, and the ratio of LUC to REN was calculated. Data represent mean ± S.E of three biological replicates. Asterisks indicate significant differences by Student *t*-test analysis (* $P \leq 0.05$; ** $P \leq 0.01$).

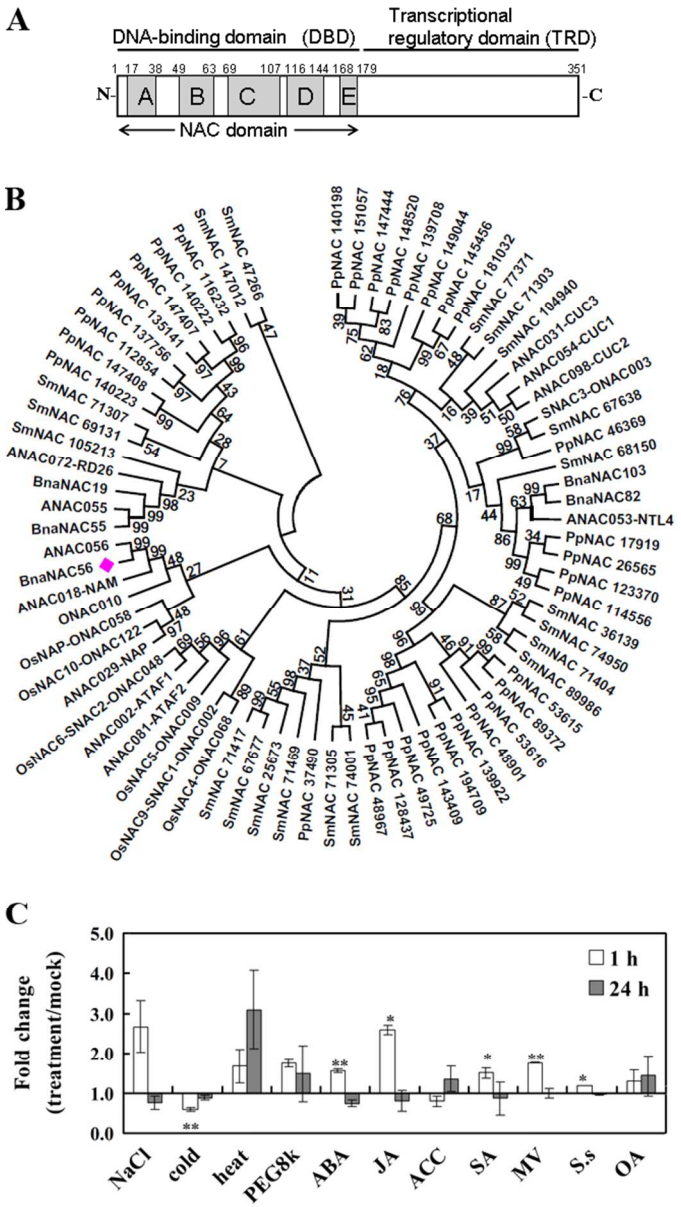

Fig. 1. Sequence and expression analysis of oilseed rape NAC56.
(A) Domain analysis of BnaNAC56. The N-terminal NAC domain and C-terminal transcriptional regulatory (TR) domain are shown, with the former divided into five conserved subdomains (A–E; shown in gray boxes). (B) Phylogenetic analysis of BnaNAC56. The tree was constructed using the maximum parsimony method implemented in MEGA6 based on amino acid sequences with BnaNAC56 indicated by a diamond. The numbers on the nodes are percentages from a bootstrap analysis of 1,000 replicates. Os, Oryza sativa; Pp, Physcomitrella patents; Sm, Selaginella moellendorffi. (C) qRT-PCR analysis of BnaNAC56 in response to various treatments. Data is the mean of three biological replicates± S.E. Asterisks denote significant differences (compared to 1) by Student t-test analysis (* p≤0.05; ** p≤0.01).

Fig. 1
80x143mm (209 x 209 DPI)

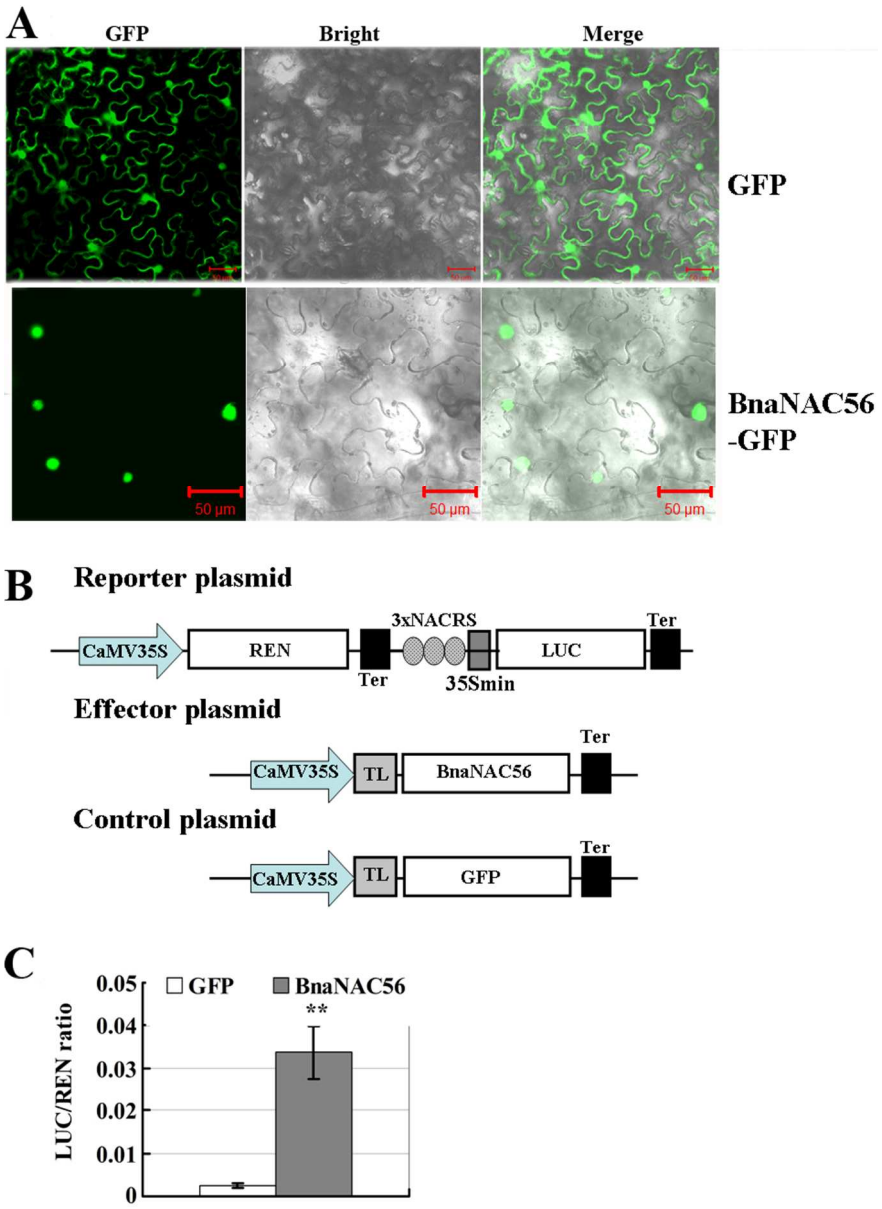

Fig. 2. Subcellular localization and transactivational activity and of BnaNAC56.
(A) Subcellular localization of BnaNAC56-GFP and GFP proteins in N. benthamiana cells. The left is GFP fluorescence, the middle bright field and the right an overlay of the two images. Bar = 50 μm. (B) Effect of BnaNAC56 on firefly luciferase (LUC) gene expression controlled by triple tandem repeats of NACRS element as revealed by dual LUC assay. GFP is the control. Asterisks denote significant differences by Student t-test analysis (** $p \leq 0.01$).

Fig. 2
100x137mm (242 x 242 DPI)

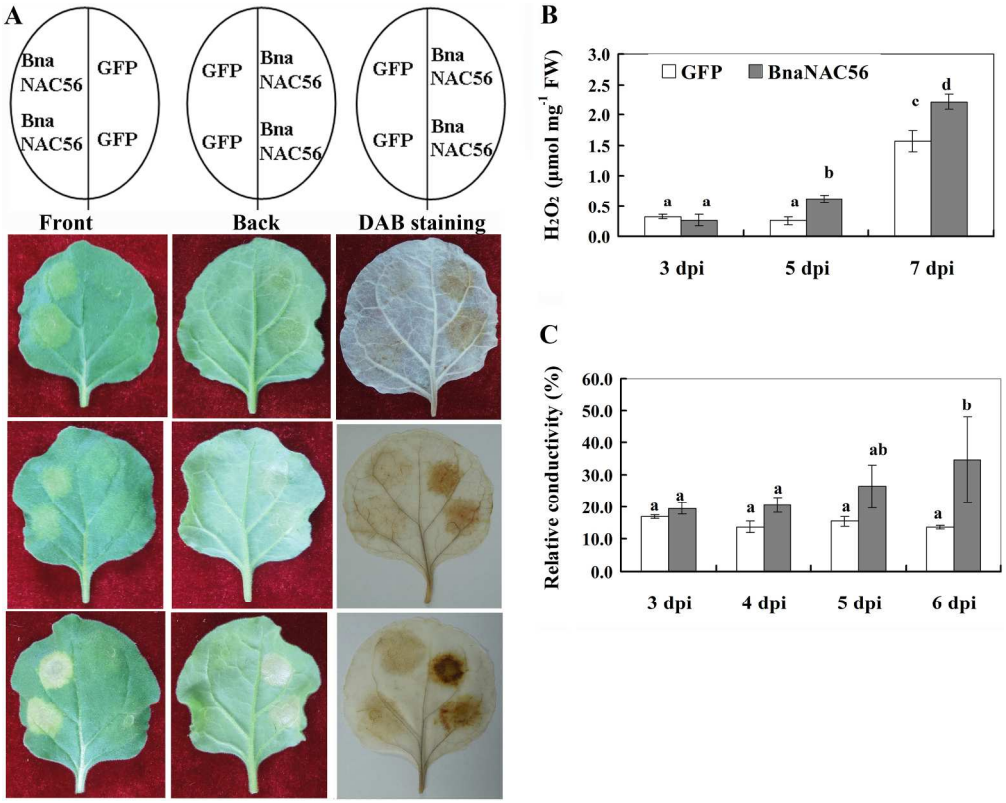

Fig. 3. Overexpression of BnaNAC56 induced ROS accumulation and HR-like cell death. (A) Cell death phenotype of N. benthamiana leaves. The diagram on the top represents the positions of infiltrated samples. The phenotype was monitored for several days post-infiltration (dpi). The left, middle and right columns represent the front, back sides and DAB staining, respectively. (B)-(C) Quantitative comparison of electrolyte leakages and hydrogen peroxide contents at various time-points, respectively. Values represent the means of three independent assays for each time-point ± S.E. Identical and different letters represent non- and significant differences ($p \leq 0.05$).

Fig. 3
111x89mm (600 x 600 DPI)

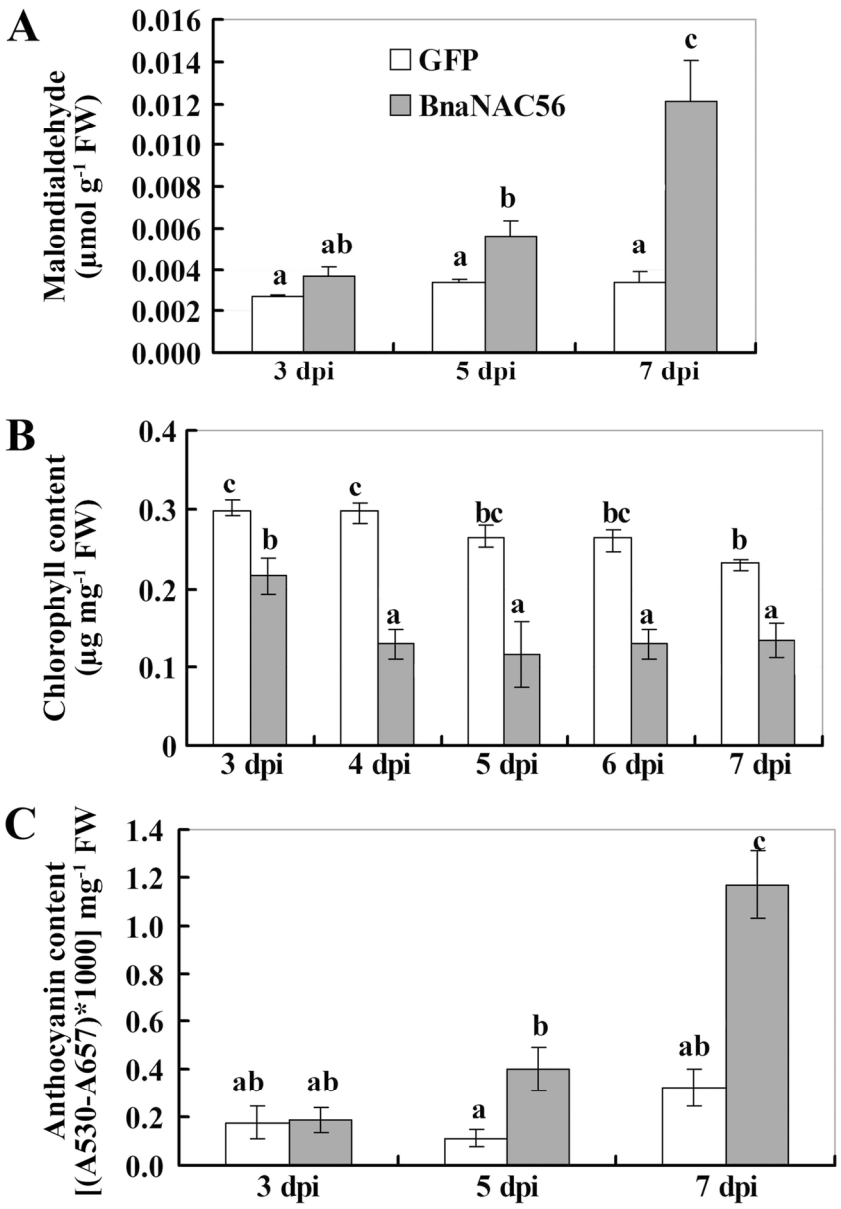

Fig. 4. Quantitative comparison of physiological indexes between BnaNAC56- and GFP-expressing tissues. (A)-(C) Quantification of MDA, chlorophyll and anthocyanin contents in leaf tissues expressing BnaNAC56 or GUS at vaious time-points. Each value is means of three independent assays± S.E. Identical and different letters represent non- and significant differences ($p \leq 0.05$).

Fig. 4
115x165mm (300 x 300 DPI)

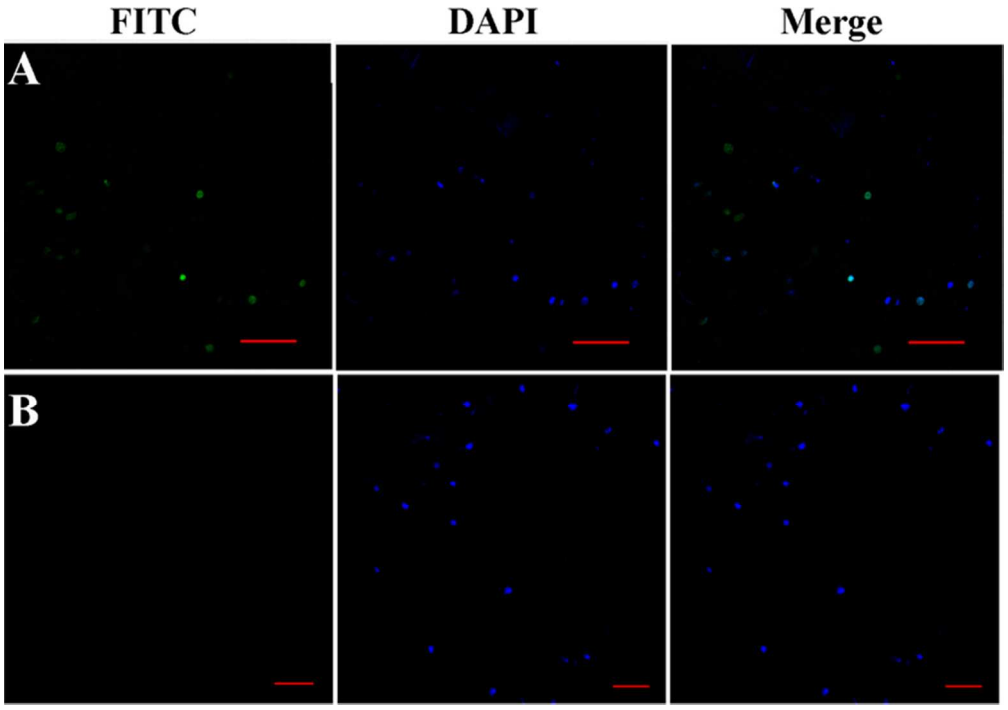

Fig. 5. Confocal images of the TUNEL assay of nuclear DNA fragmentation induced by BnaNAC56 expression. (A) and (B), Images of leaves expressing BnaNAC56 and GUS at 5 dpi, respectively. Leaves were counterstained with DAPI. Scale bars = 20 μm.
Fig. 5
69x48mm (300 x 300 DPI)

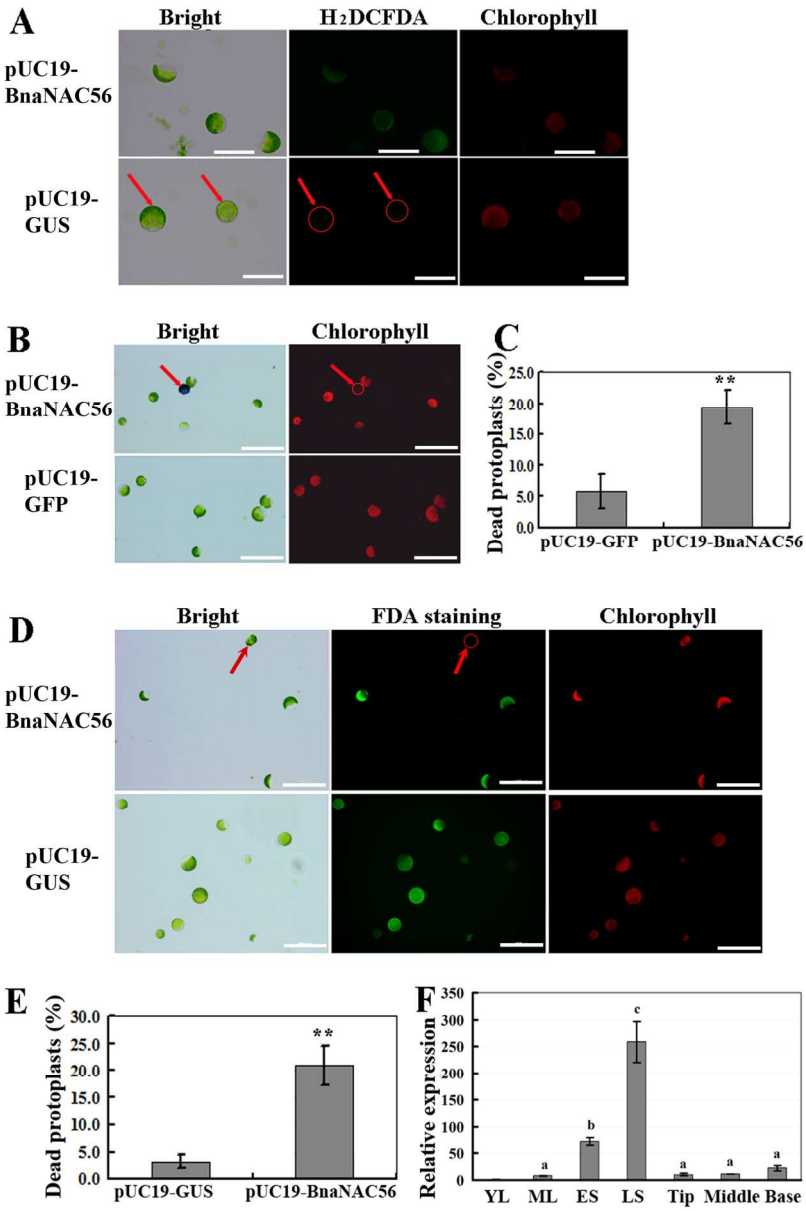

Fig. 6. Expression of BnaNAC56 in protoplasts OF oilseed rape induced cell death. (A) Detection of cell death. Protoplasts were transfected with the pUC19-BnaNAC56 and pUC19-GFP (control) plasmids, respectively. After 18 h, viability of protoplasts was assayed. Red circless indicate dead protoplasts. (B) Percentages of dead protoplasts. Values were means of 20 independent assays ± S.E. (C) qRT-PCR analysis of BnaNAC56 expression during leaf senescence. YL, young leaves; ML, mature leaves; ES, early senescent leaves; LS, late senescent leaves; T, M and B indicate tip, middle and base of ES senescent leaves. Data is the mean of three biological replicates± S.E.

Fig. 6
180x270mm (300 x 300 DPI)

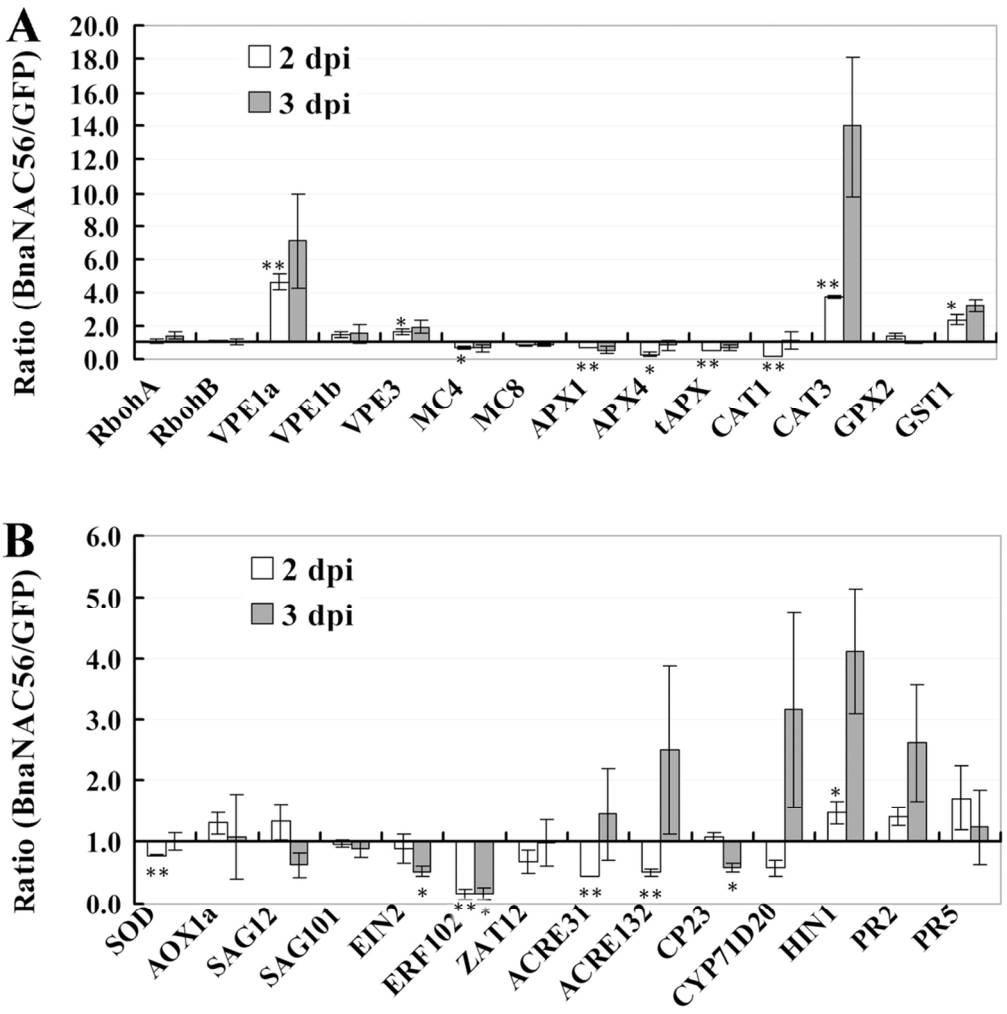

Fig. 7. qRT-PCR analysis of transcript abundance of ROS-, cell death- and defense-related marker genes. (A) and (B) qRT-PCR was performed to determine transcript levels of marker genes in control and BnaNAC56-expressing leaves at 2 and 3 dpi. Each value represents the mean ± S.E. of three biological replicates. Asterisks denote significant differences (compared to 1) by Student t-test analysis (* $p \leq 0.05$; ** $p \leq 0.01$).

Fig. 7
99x99mm (300 x 300 DPI)

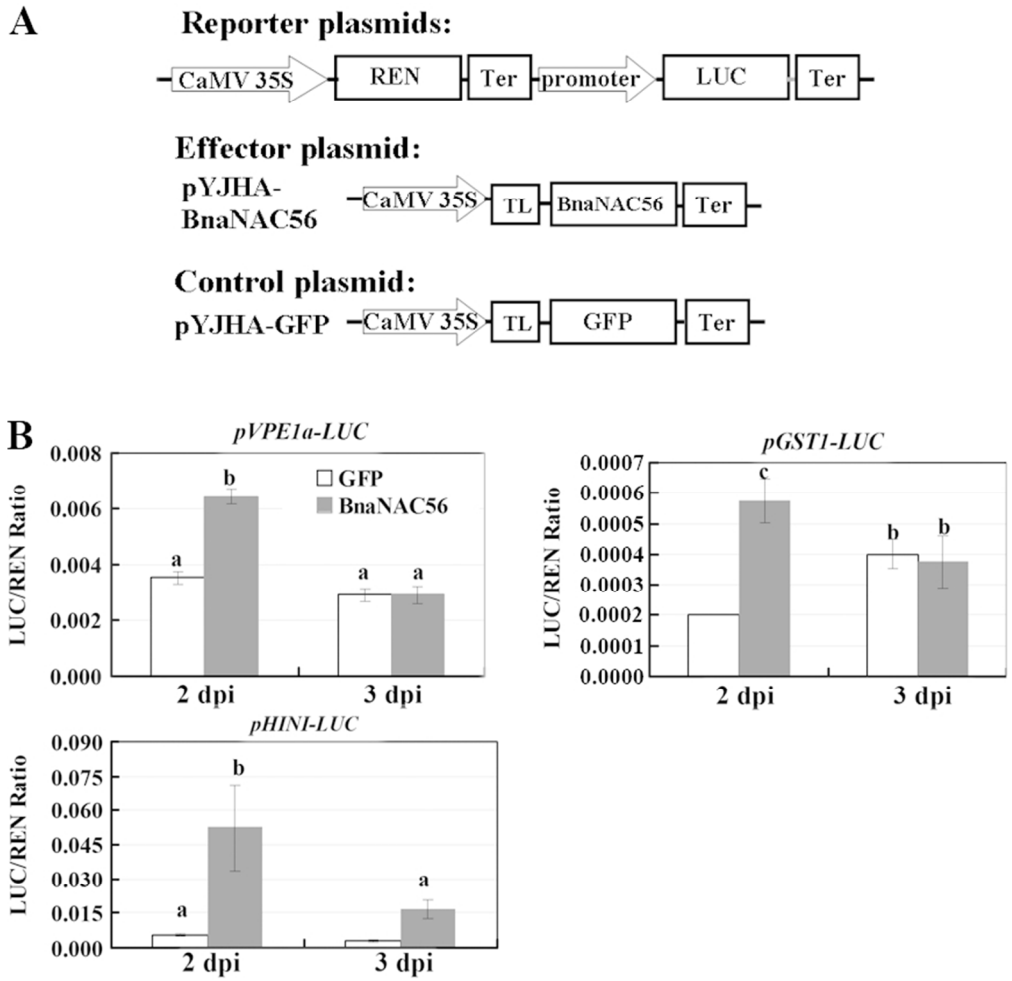

Fig. 8. The dual luciferase reporter assay of transcription activation of BnaNAC56.
(A) Schematic representation of the double-reporter and effector plasmids used in the dual LUC assay. The double-reporter plasmid contains the respective promoter regions fused to LUC and Renilla (REN) luciferase driven by CaMV35S. The effector plasmid contains the BnaNAC56 driven by the CaMV35S. TL, translational leader sequence from tobacco etch virus; Ter, NOS terminator. (B) Ability of BnaNAC56 to activate expression of LUC under the control of various promoter regions. The activities of LUC and REN were measured sequentially, and the ratio of LUC to REN was calculated. Data represent mean ± S.E of three biological replicates. Asterisks indicate significant differences by Student t-test analysis (* $p \leq 0.05$; ** $p \leq 0.01$).

Fig. 8
120x117mm (182 x 182 DPI)